ORIGINAL ARTICLE

No imprinted *XIST* expression in pigs: biallelic *XIST* expression in early embryos and random X inactivation in placentas

Huiying Zou[1,2] · Dawei Yu[3] · Xuguang Du[2] · Jing Wang[2] · Lei Chen[4] · Yangyang Wang[1] · Huitao Xu[1] · Yunxuan Zhao[3] · Shanjiang Zhao[1] · Yunwei Pang[1] · Yan Liu[1] · Haisheng Hao[1] · Xueming Zhao[1] · Weihua Du[1] · Yunping Dai[2] · Ning Li[2] · Sen Wu[2,5] · Huabin Zhu[1]

Abstract

Dosage compensation, which is achieved by X-chromosome inactivation (XCI) in female mammals, ensures balanced X-linked gene expression levels between the sexes. Although eutherian mammals commonly display random XCI in embryonic and adult tissues, imprinted XCI has also been identified in extraembryonic tissues of mouse, rat, and cow. Little is known about XCI in pigs. Here, we sequenced the porcine *XIST* gene and identified an insertion/deletion mutation between Asian- and Western-origin pig breeds. Allele-specific analysis revealed biallelic *XIST* expression in porcine ICSI blastocysts. To investigate the XCI pattern in porcine placentas, we performed allele-specific RNA sequencing analysis on individuals from reciprocal crosses between Duroc and Rongchang pigs. Our results were the first to reveal that random XCI occurs in the placentas of pigs. Next, we investigated the H3K27me3 histone pattern in porcine blastocysts, showing that only 17–31.8% cells have attained XCI. The hypomethylation status of an important *XIST* DMR (differentially methylated region) in gametes and early embryos demonstrated that no methylation is pre-deposited on *XIST* in pigs. Our findings reveal that the XCI regulation mechanism in pigs is different from that in mice and highlight the importance of further study of the mechanisms regulating XCI during early porcine embryo development.

Abbreviations

DMR	Differentially methylated region
E	Embryonic day
H3K27me3	Histone H3 lysine 27 trimethylation
ICSI	Intracytoplasmic sperm injection
ICR	Imprinting control region
IVF	In vitro fertilization
Xic	X inactivation center
PA	Parthenogenetic
PRC2	Polycomb repressive complex-2
RFLP	Restriction fragment length polymorphism

✉ Sen Wu
swu@cau.edu.cn

✉ Huabin Zhu
zhuhuabin@caas.cn

1   Key Laboratory of Animal (Poultry) Genetics Breeding and Reproduction, Ministry of Agriculture and Rural Affairs, Institute of Animal Science, Chinese Academy of Agricultural Sciences, Beijing 100193, China

2   State Key Laboratory of Agrobiotechnology, College of Biological Sciences, China Agricultural University, Beijing 100193, China

3   State Key Laboratory of Stem Cell and Reproductive Biology, Institute of Zoology, Chinese Academy of Sciences, Beijing 100101, China

4   Chongqing Academy of Animal Science, Chongqing 402460, China

5   Beijing Advanced Innovation Center for Food Nutrition and Human Health, China Agricultural University, Beijing 100193, China

SNP	Single nucleotide polymorphism
TSS	Transcription start site
TTS	Transcription termination site
Xa	Active X chromosome
XCI	X-chromosome inactivation
Xi	Inactive X chromosome
XIST	X-inactive specific transcript
Xm	Maternal X chromosome
Xp	Paternal X chromosome

Introduction

Sex is determined by the sex chromosome complement in placental mammals: XY in males and XX in females. Sex chromosomes evolve into a relatively large, gene-rich X chromosome and a small, gene-poor Y chromosome (reviewed in Ref. [1]). Genes on the X chromosome are present in one copy in males and two copies in females. Thus, to ensure dosage compensation of X-linked genes in female mammals, the expression of genes on one of the X chromosomes is repressed via X-chromosome inactivation (XCI) [2–4].

There are two modes of XCI: random and imprinted. Nearly all eutherian mammals appear to undergo random XCI in their soma, whereas marsupials show paternal imprinted XCI (reviewed in Ref. [5]). However, preimplantation embryos and extraembryonic tissues of mice exhibit imprinted XCI [6]. XCI initiation is regulated by the X inactivation center (*Xic*), a master regulatory locus that harbors the main XCI regulator, and the long noncoding RNA *Xist* ([7], reviewed in Refs. [8, 9]). *Xist* RNA is exclusively expressed from and preferentially coats the inactive X-chromosome in cis (reviewed in Ref. [10]). Xist coating is followed by recruitment of multiple chromatin-modifying complexes such as polycomb repressive complex-2 (PRC2), which trimethylates lysine 27 on histone H3 (H3K27me3), repressing X-linked gene expression (reviewed in Refs. [11, 12]). In mice, *Xist* produces a 17-kb noncoding transcript whose accumulation on X chromosomes (Xist coating) has been associated with the initiation of both random and imprinted XCI [13]. During early mouse embryogenesis, paternal *Xist* is expressed from the two- to four-cell stage, and the maternal *Xist* allele is repressed until the morula stage [14, 15]. The paternal X chromosome (Xp) becomes inactivated, and XCI gradually occurs in the developing extraembryonic lineages and is maintained in the placenta (imprinted XCI). In contrast, the Xp–Xist coating (accumulation of *Xist* RNA on the Xp) in epiblast cells is lost and the Xp becomes reactivated [16]. The second round of XCI then occurs in the developing embryonic tissues at approximately embryonic day (E) 5.5, and the Xp and maternal X chromosomes (Xm) have equal chances of becoming inactivated (random XCI) (reviewed in Ref. [17]).

Mice are the only eutherian mammals in which XCI during early embryogenesis has been analyzed in detail. Imprinted X inactivation has also been reported in rat yolk sacs [18] and bovine placenta [19], but no imprinted inactivation of Xp was found to occur in the trophectoderm of female bovine blastocysts [20]. In horse placentas, random X inactivation has been found to occur [21]. Furthermore, XCI was not observed in monkey preimplantation embryos [22]. What is more, partial expression dampening of the two X chromosomes was observed in preimplantation embryos in humans [23] and naïve human pluripotent stem cells [24]. However, this strategy for dosage compensation remains controversial in humans [25, 26]. Little is known about the XCI status in the placentas of other mammals such as pigs. A clear association has been reported between the failure of the development of cloned embryos and the aberrant patterns of XCI in mice [27] and cows [19]. XCI status has also been used as a marker to determine the naïve and primed status of pluripotent stem cells [28]. Although the importance of XCI status has been highlighted in various fields of research, only some studies have investigated XCI in pigs [29, 30]. Park et al. [31] studied normal fertilized and uniparental porcine embryos and reported that imprinted *XIST* expression occurs in preimplantation embryos. However, their findings require further validation by more direct evidence such as allele-specific expression analysis.

Allele-specific expression analysis of X-linked genes is used to determine whether imprinted XCI occurs in the placentas of different species [21, 32, 33]. To determine the allele-specific expression status of X-linked genes, suitable polymorphic markers are required to distinguish between maternal and paternal alleles. A vast number of different single nucleotide polymorphisms (SNPs) have been reported in swine breeds of Asian and Western origins; these have been used as a powerful tool to study imprinted genes in pigs [34–36]. Here, we performed a genome comparison to identify different SNPs in the X-linked genes between domestic Duroc and Rongchang pigs (a local Chinese pig breed). Based on these X-linked SNPs, we analyzed the allele-specific gene expression along the X chromosome in placentas from reciprocal crosses between the two distinct breeds.

Materials and methods

Sample preparation, RNA extraction, and reverse transcription

Total RNA was extracted from placentas of hybrids and hybrid (R-D) fibroblasts using TRIzol Reagent (ComWin

Biotech) and purified with the RNAeasy Mini Kit (Qiagen). RNA (2 µg) was reverse transcribed using M-MLV reverse transcriptase (Promega). XIST SNP amplicons were produced using the primer pair XIST-SNP-F/R. XIST SNP amplicons from Duroc pigs were 428 bp in length and could be digested into 299- and 136-bp fragments by *Ava*II. XIST SNP amplicons from Rongchang pig were 428 bp in length, contained a 7-bp deletion, and could not be digested by *Ava*II.

Single embryos were washed twice in phosphate-buffered saline (PBS) and collected in 2.5-µL cold Cell Lysis II Buffer (Cells-to-cDNA™ II Kit, Invitrogen). Lysates were stored at −80 °C until use. Single embryos were reverse transcribed using Cells-to-cDNA™ II Kit (Invitrogen) without isolating RNA. The cDNA produced was used for the subsequent polymerase chain reaction (PCR). As little cDNA existed, we designed nested primer pairs XISTouter-SNP-F/R and XIST-SNP-F/R. PCR products were digested by *Ava*II.

RACE-PCR of 5′- and 3′-regions

To determine the location of the transcription start site (TSS) in *XIST*, we mapped the TSS using a 5′-rapid amplification of cDNA ends (RACE) system (Invitrogen). Three gene-specific primers, 5RACE-549R, 5RACE-773R, and 5RACE-856R, were designed using the obtained 5′-upstream XIST sequence. RNA was extracted from the liver of Duroc pigs. We performed 5′-RACE in accordance with manufacturer's instructions. The PCR products were cloned into pMD19-T vector (TaKaRa) and sequenced.

We performed 3′-RACE to determine the location of the *XIST* transcription termination site (TTS). Three gene-specific primers, 3RACE 31074F, 3RACE 31171F, and 3RACE 31324F, were designed using the obtained 3′-downstream XIST sequence. RNA was extracted from the livers of Duroc pigs. The 3′-RACE system (Invitrogen) was used in accordance with the manufacturer's instructions. Amplification conditions were as follows: 94 °C for 5 min, 94 °C for 30 s, 58 °C for 30 s, and 72 °C for 1 min. The obtained PCR products were cloned into pMD19-T vector (TaKaRa) and sequenced.

In vitro maturation (IVM)

Ovaries were collected from prepubertal cross-bred gilts (Landrace, Large White, and Duroc breeds) at a local slaughterhouse. The collected ovaries were then transported to the laboratory at 37 °C within 2 h. Cumulus–oocyte complexes (COCs) were collected from antral follicles of 2–6 mm in diameter using 18-gauge needles and washed twice with TL–Hepes–PVA medium. After washing, the COCs were matured in groups of 50–60 in 500-µL maturation medium [37], and cultured in dishes of a four-well plate (Nunclon) for 42–44 h. After maturation, the cumulus cells were removed from the oocytes by treatment with 0.1% hyaluronidase (Sigma) and gently pipetted for 2 min. Denuded oocytes with the first polar body were selected and used as in vitro matured oocytes.

Parthenogenesis (PA)

Cumulus-free oocytes were equilibrated for 10 s in the activation medium (280 mM mannitol solution containing 0.5 mM Hepes, 0.1 mM $CaCl_2$, and 0.1 mM $MgCl_2$). Treated oocytes were then placed in an electrode chamber and activated with a single DC pulse (1.2 kV/cm 100 µs) using an electrofusion instrument (CF-150B; BLS, BP, Hungary). The activated oocytes were cultured in PZM-3 supplemented with 5 µg/mL cytochalasin B and 10 µg/mL cycloheximide for 4 h, then washed thoroughly three times, and cultured again in PZM-3 at 38.5 °C in 5% CO_2, 5% O_2, and 90% N_2 with maximum humidity.

Intracytoplasmic sperm injection (ICSI)

Ejaculated semen samples were collected from boars of the Rongchang breed. Sperm cryopreservation and injection were carried out as described previously [38, 39]. Cryopreserved spermatozoa were thawed in DPBS supplemented with 1 mg/mL bovine serum albumin (BSA) at 37 °C, and washed three times. The sperm pellet was resuspended in pig fertilization medium with 5 mg/mL BSA. A small volume (0.5 µL) of the sperm suspension was transferred to a 2-µL drop of IVC–PyrLac–Hepes–PVP. Approximately 20–30 oocytes were transferred to a 20-µL drop of IVC–PyrLac–Hepes, which was prepared close to the drops used for the sperm. Single spermatozoa were picked and injected into each ooplasm using a Piezo-actuated micromanipulator. After artificial stimulation, which was the same procedure as that used for parthenogenesis, sperm-injected oocytes were cultured in PZM-3 at 38.5 °C in 5% CO_2, 5% O_2, and 90% N_2 with maximum humidity.

Primary cell isolation and culture

Ear tissues were obtained from newborn piglets of Duroc sows and Rongchang boars and treated with 75% ethanol for 5 min and washed three times with PBS containing 2% penicillin–streptomycin. Fibroblasts were isolated from ear skin biopsy and cultured in Dulbecco's modified Eagle's medium (Gibco) supplemented with 10% fetal bovine serum (Gibco) in a humidified incubator at 37.5 °C in the presence of 5% CO_2.

Allelic expression of X chromosome genes in primary fibroblast cell lines

We used the SNPs to decide the allele assignment of sequencing reads for the parental alleles. The genes which contained informative reads were designated as testable. Then, we used all the parental reads to calculate parental expression of the testable genes. We calculated the expression ratio of the X-linked genes between the active X and inactive X alleles and used the ratio of 0.1 as a threshold to define the inactivation and escape X-inactivation genes.

Allele-specific RT-PCR analysis

Several X-linked genes containing different SNP sites in Duroc and Rongchang pigs were screened in RNA-seq data from F1 hybrids of Duroc sows and Rongchang boars. Information for primers and SNP positions is available in Table S1 and Table S2. PCR was performed in cDNAs of the F1 hybrid placentas and R-D cells, isolation from newborn piglets of Duroc sows and Rongchang boars. The obtained PCR products were sequenced. X-linked genes with double peaks at SNP sites indicated that they were expressed from two alleles. Genes exhibiting single peaks at SNP sites in R-D cell lines indicated that one of the alleles were subject to inactivation.

Bisulfite genomic sequencing analysis

Genomic DNA was extracted from tissue samples using a standard two-step phenol–chloroform extraction method. For bisulfite genomic sequencing, 500 ng of gDNA was subjected to bisulfite treatment using a MethylDetector™ Bisulfite Modification Kit (Active Motif), according to the manufacturer's protocol. Bisulfite sequencing PCR primers were designed using a web-based Methyl Primer tool (http://www.urogene.org/cgi-bin/methprimer/methprimer.cgi). Information about the primers used is available in Table S1. The PCR products were cloned into pMD19-T vector. At least ten randomly selected clones were sequenced. The sequences were aligned using a web-based quantification tool for methylation analysis (QUMA; http://quma.cdb.riken.jp/).

Immunofluorescence

Immunofluorescence was carried out as described previously [40]. Cells and embryos were permeabilized in PBS-0.5% Triton-X100 for 5 min and fixed in 4% paraformaldehyde (in $1 \times$ PBS, pH 7.4) for 10 min at room temperature. After blocking in 0.1% Triton X-100 and 2% BSA-supplemented PBS for 1 h, the cells and embryos were incubated with primary antibodies overnight at 4 °C. They were then washed three times with 0.05% Tween-PBS and incubated with secondary antibodies for 1 h at 37 °C. After washing three times in PBS, they were counterstained with DAPI (Invitrogen) and mounted on glass slides. Finally, the slides were examined under a confocal laser-scanning microscope (C-1, Nikon). Anti-histone H3K27me3 antibodies (Abcam) were diluted 200 times. Goat anti-rabbit IgG coupled to Alexa Fluor-488/594 (Invitrogen) were used in a 1:1000 dilution.

Analysis of allele-specific expression patterns of X-linked genes in the placenta

To investigate the allele-specific expression patterns on the X chromosome in pig placentas, we analyzed RNA-seq data from hybrid placenta from the progeny of reciprocal crosses [41]. The placentas were obtained on day 20 of pregnancy. The parental origins of the two alleles in the hybrids were distinguished using heterozygous SNPs (which were homozygous in the parents) identified from whole genome resequencing of their parents from the previous study [42].

Clean reads were aligned to their respective parental genomes using Hisat [43]. All the subsequent sequencing analyses were conducted on the basis of the average result mapped to the parental genome.

Heterozygous SNPs of hybrids were retained by identifying the pure SNP between its maternal and paternal genome. A total of 306,634 SNPs were obtained in each hybrid individual to determine the parental origin of each allele on the X chromosome. To assign each read to its parental origin, all SNPs in the read with high-quality base calling (Phred score ≥ 20). When multiple SNPs were present in a read (or a read pair), the origin was determined by votes from all SNPs and the read was assigned to the allele that had at least half of the total votes. The number of reads assigned to each paternal allele was then determined and normalized using HT-seq (v0.5.3.p3) [44].

Results

Identification of the full-length RNA sequence of porcine *XIST*

We used two known porcine ESTs (EF619477.1 and AJ429140.1) to perform a BLAST search against the porcine nucleotide collection (nr/nt) database, and identified BAC CH242-76N1 (GI: 219925014), which contained the porcine *XIST* gene. Then, we aligned and compared BAC CH242-76N1 with human *XIST* RNA (NR_001564). The candidate porcine *XIST* gene ranged from 289,233 to 257,103 nucleotides in the DNA sequence. Meanwhile, four important homologous regions ($-113,947 - 111,847$; $-103,486 - 103,622$; $-105,757 - 105,551$; $-103,318 - 102,531$)

were found, and the homologous regions in human *XIST* RNA span from exons 1–6. We assumed that the homologous regions in BAC CH242-76N1 contain all exon/intron junction sites of porcine *XIST* RNA. Primers were designed according to the homologous regions. Table S1 contains information about the primers used. RT-PCR was performed using cDNA from female Duroc pigs (Fig. S1A). Twelve exon/intron junction sites were found from the cDNA sequences that were aligned with the BAC CH242-76N1 sequence.

We next designed 14 pairs of overlapping primers based on the candidate porcine *XIST* gene excluding the homologous regions (Table S1). The genomic DNA and cDNA were used as templates to amplify these fragments. The corresponding bands that were amplified in cDNA and genome were all the same size, suggesting that the amplified regions were all exons (Fig. S1B). The PCR products were sequenced to identify the exact sequence of *XIST* RNA in Duroc pigs.

To identify the TSSs of porcine *XIST*, 5′-RACE was performed using the primers listed in Table S1 (Fig. S1C). Nucleotide 129,032 of BAC CH242-76N1 was determined to be a TSS of porcine *XIST* by sequencing, and it has been suggested to be conserved in the *XIST* minimal promoter region among murine, bovine, and human genomes. Moreover, another TSS was identified at +104. Furthermore, 3′-RACE was conducted to identify the TTS of porcine *XIST* (Fig. S1C). Sequencing analysis revealed that nucleotide 96,366 of BAC CH242-76N1 was the porcine TTS of *XIST*.

We successfully identified the porcine *XIST* gene encoding a 25,065-bp transcript consisting of seven exons. The A-repeats, which are the most important region of the *XIST* RNA for silencing the X chromosome, have 8 copies of a 24-bp consensus sequence ranging from +328 to +696 in the porcine *XIST* RNA.

A conserved *XIST* SNP among Asian- and Western-origin swine breeds

We compared the genomes of Western and Asian pig breeds and found a 7-bp (TCCATGG) insertion (Western pig)/deletion (Asian pig) mutation at position 19,088 of the *XIST* RNA (Fig. 1a–c). The mutation could be detected using the restriction enzyme *Ava*II. The primer pair XIST-SNP-F/R was used to amplify a 435/428-bp fragment containing the mutation of the *XIST* gene from both Asian and Western pigs (Table S1). The PCR products of Western pigs could be digested by *Ava*II to obtain 299- and 136-bp fragments, whereas the 428-bp PCR products of Asian pigs could not be digested. To validate the mutation of the *XIST* gene in different pig breeds, we analyzed tissues from Landrace, Large White, Duroc, Erhualian, Xiang, and Rongchang pigs. Restriction fragment length polymorphism (RFLP) analysis
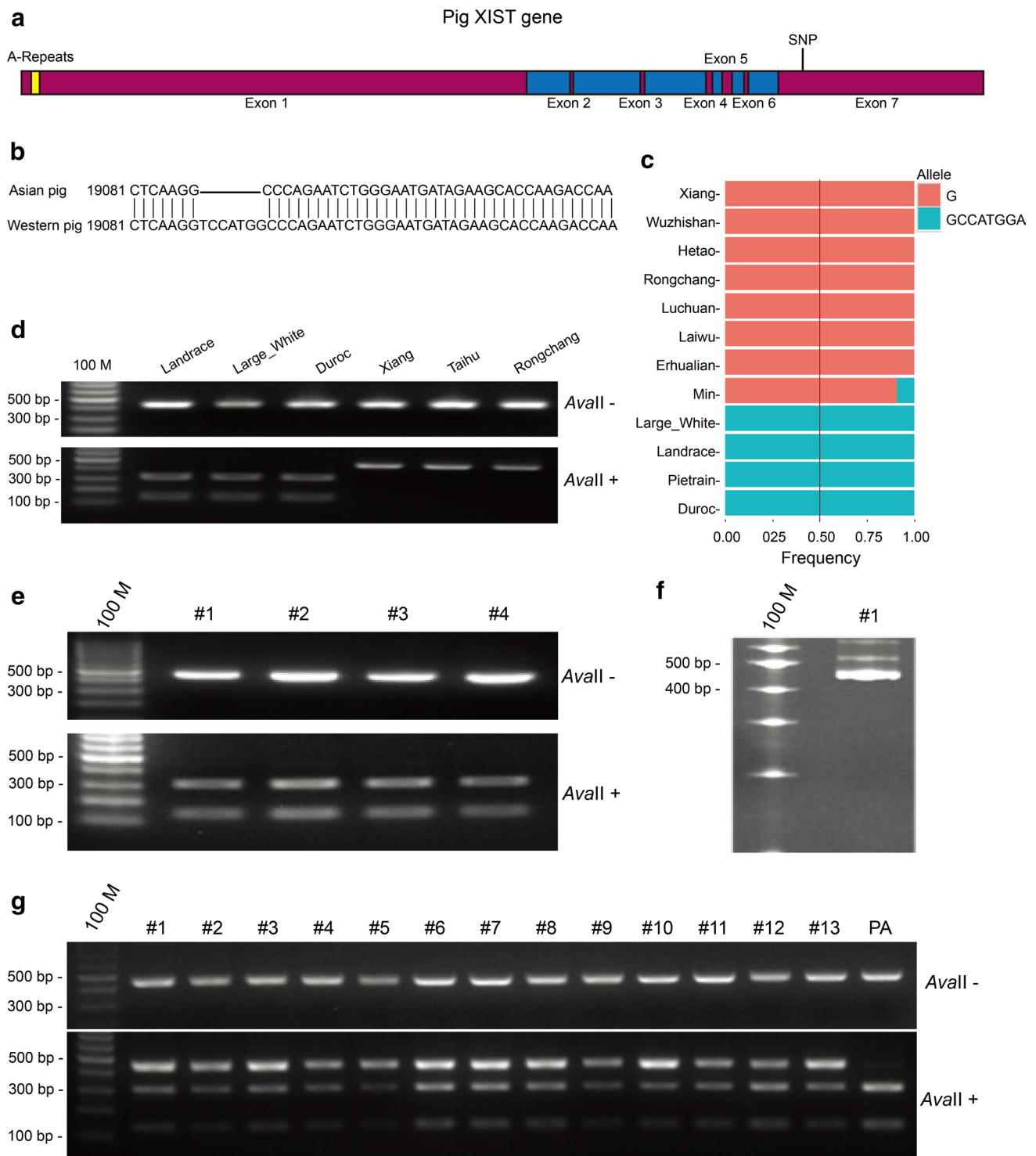
of the PCR products revealed an insertion mutation in the *XIST* gene in Landrace, Large White, and Duroc pigs, and a deletion mutation in the *XIST* gene in Erhualian, Xiang, and Rongchang pigs (Fig. 1d). This was further confirmed by sequencing analysis of the PCR products.

Biallelic *XIST* expression in early porcine ICSI embryos

To determine the allele-specific expression status of the *XIST* gene in early porcine embryos, the insertion/deletion mutation was used as a polymorphic marker to distinguish between maternal and paternal alleles. Oocytes collected from the ovaries of cross-bred gilts (Landrace, Large White, and Duroc breeds) contained the *XIST* insertion mutation, which was confirmed by RFLP analysis of cumulus cells (Fig. 1e). The sperm collected from Rongchang boars contained a deletion in the *XIST* gene, which was also confirmed by RFLP analysis (Fig. 1f). To circumvent the high polyspermy rates following in vitro fertilization (IVF) embryos in pigs, ICSI was conducted. We then detected the allele-specific expression status of the *XIST* gene in single female E6 blastocysts. RT-RFLP analysis indicated that both paternal and maternal alleles of the *XIST* gene were expressed in all the female ICSI embryos (Fig. 1g).

Confirmation of X-linked genes which are subject to XCI

To address whether a particular X-linked gene is subject to X inactivation or escapes from it, X-linked gene polymorphisms were used to distinguish between Xa and Xi expression in clonal cell lines from heterozygous individuals [45]. Primary fibroblast cells used for this study were derived from F1 female hybrids of Duroc sows and Rongchang boars. Clonal cell lines were established from the expansion culture of single fibroblast cells. SNPs of three X-linked genes, *G6PD*, *HPRT1*, and *ZBTB33*, whose X inactivation status in mice and humans has been confirmed, were identified in the Duroc and Rongchang pig genomes (Fig. 2a). Results of the genome comparison revealed a G-T (Rongchang–Duroc) mutation at position 1119 (XM_003360515) of the *G6PD* gene, a C-A (Rongchang–Duroc) mutation at position 397 (NM_001032376) of the *HPRT1* gene, and a C-T (Rongchang–Duroc) mutation at position 4910 (XM_003135334) of the *ZBTB33* gene (Table S2). Primer pairs (G6PD-F/R, HPRT1-F/R, and ZBTB33-F/R) were used to amplify fragments containing the mutations of the *G6PD, HPRT1,* and *ZBTB33* genes, respectively, from the cDNA of three clonal cell lines. Results of the sequencing of the RT-PCR products showed monoallelic expression of *G6PD, HPRT1,* and *ZBTB33* in all three heterozygous clonal cell lines

a

b

Asian pig   19081 CTCAAGG————————CCCAGAATCTGGGAATGATAGAAGCACCAAGACCAA
                         | | | | | | | | | | | | | | | | | | | | | | | | | | | | | | | | | | | | | | | | | | | | |
Western pig 19081 CTCAAGGTCCATGGCCCAGAATCTGGGAATGATAGAAGCACCAAGACCAA

c

d

e

f

g

(Fig. 2b), which is consistent with the RT-RFLP analysis of *XIST*. This finding demonstrates that *XIST* is expressed only from Xi chromosomes in these clonal cell lines (Fig. 2c). Altogether, these results indicate that the *G6PD, HPRT1*, and *ZBTB33* are subject to X inactivation in porcine somatic cells, which pave the way for studying the pattern of X inactivation in the porcine placenta.

We took three other clonal cell lines for RNA sequencing to analyze X chromosome-wide profiling of X-linked gene expression (Fig. S2). A gene whose expression ratio from Xi and Xa was more than 10% (allelic ratio > 0.1) was identified as an escape gene. Among the 1120 genes on the X chromosome in the pig (Ensembl), 144 genes contained SNPs were detected in the three clonal cell lines (Table S3).

◄**Fig. 1** Identification of a conserved SNP in the porcine *XIST* genes between Asian and Western pigs and *XIST* expression in early female porcine ICSI embryos. **a** Schematic depicting the porcine *XIST* gene structure. Porcine *XIST* gene transcripts a 25,065 bp *XIST* RNA consisting of seven exons, with large exons 1 and 7 and five small exons. Relative lengths of each exon are 17,185 bp, 89 bp, 136 bp, 209 bp, 329 bp, 129 bp and 6988 bp. The yellow-labeled element is A-Repeats. **b** Location and insertion/deletion mutation of the conserved SNP between Asian and Western pigs. A 7-bp (TCCATG G) insertion exists in the *XIST* RNA of Western pigs. **c** Analysis of the frequency of the *XIST* SNP among different breeds of Asian and Western pigs. *XIST* RNAs of Xiang, Wuzhishan, Hetao, Rongchang, Luchuan, Laiwu, and Erhualian pigs have a 7-bp (TCCATGG) deletion, while the *XIST* RNA of Large White, Landrace, Pietrain, and Duroc pigs have a 7-bp (TCCATGG) insertion. **d** Validation of the *XIST* SNP in some pig species by digestion with *Ava*II. PCR products from Western pigs are digested by *Ava*II to 299-bp and 136-bp fragments, whereas PCR products from Asian pigs cannot be digested by *Ava*II. **e** Polymorphism of *XIST* in granulosa cells shed from COCs used to produce ICSI embryos. Ovaries were obtained from pigs in a slaughterhouse and used to produce ICSI embryos. PCR products of granulosa cells were digested by *Ava*II. **f** Polymorphism of *XIST* in Rongchang pig sperms used to produce ICSI embryos. The PCR products of sperms cannot be digested by *Ava*II. **g** Digestion of RT-PCR products from female porcine ICSI embryos. The PCR procucts were partially digested by *Ava*II, indicating that *XIST* is randomly expressed from the paternal or maternal X chromosome. The genome of PA (parthenogenetic embryo) is entirely from the mother. Therefore, the RT-PCR procucts of parthenogenetic embryos can be totally digested by *Ava*II

Twenty-two genes were detected to escape X inactivation in all three clonal cell lines, with variable expression from Xi, while 122 genes were subject to X inactivation (Table S3). Some genes were subject to inactivation in two clonal cell lines but escaped from inactivation in one clonal cell line, which indicated that three clonal cell lines have considerable heterogeneity in X-linked gene expression (Fig. S2).

Random X inactivation in porcine placenta

To investigate the X inactivation pattern in porcine placentas, we carried out RNA sequencing of female hybrid placentas of Duroc and Rongchang pigs [41]. SNPs were available in 307 expressed genes for allelic analysis. The expression ratios of X-linked genes in maternal and paternal X chromosomes are nearly 1:1 (Figs. 3a and S3). No allele-specific expression was detected on the X-chromosome (binomial test, $P < 0.05$). We then examined the distributions of allele-specific expression of the *XIST*, *G6PD*, *HPRT1*, and *ZBTB33* genes in placenta samples of female hybrids of Duroc sow and Rongchang boar. In three female placenta samples, the *G6PD*, *HPRT1,* and *ZBTB33* genes exhibited biallelic expression (Fig. 3b), which was associated with the biallelic expression of the *XIST* gene. The expression ratio of *XIST* from the paternal allele is 35–76% (Fig. 3c). These results indicated that random XCI occurred in porcine placentas.

XCI status in early porcine embryos produced in vitro

H3K27me3 enrichment has been shown to be a characteristic of the inactivation process of the X-chromosome. To investigate the XCI process in early porcine embryos, we performed immunostaining to examine the nuclear profiles of H3K27me3 enrichment in ICSI and parthenogenetic (PA) embryos at E7 blastocyst stage (Fig. 4a). Of 15 ICSI embryos analyzed at the E7 blastocyst stage, 8 were male embryos because the H3K27me3 signal in these embryos was absent or weakly positive. Two of the 8 male embryos displayed one dense H3K27me3 signal in 1.6–3.4% of the nuclei (Fig. 4b). In 7 female ICSI embryos, 17–31.8% cells had one H3K27me3 signal (Fig. 4b). Two H3K27me3 staining spots in each nucleus could sometimes be observed in ICSI embryos (1.2–5.7%) (Fig. 4b). All 6 of the E7 PA embryos analyzed showed one dense H3K27me3 domain in 7.1–9.5% of the nuclei. Two H3K27me3 staining spots per nucleus were also detected in 1.9–7.1% of PA embryos (Fig. 4c). In some E7 ICSI embryos, H3K27me3 enrichment in one and two domains in the nucleus was colocalized, suggesting that XCI has initiated but not accomplished in porcine E7 blastocysts (Fig. 4a), which was in agreement with the latest research [46]. The nuclear profiles of H3K27me3 enrichment in E7 PA embryos were found to be similar to those in ICSI embryos, which were consistent with the expression of *XIST* in PA embryos, indicating that imprinting may not play a major role in porcine XCI.

Analysis of *XIST* differential methylated region (DMR)

In a previous study in mice, the methylation pattern of the *XIST* promoter region was highly related to its imprinted expression during preimplantation embryo development [47]. The expression of imprinted genes is generally controlled by CpG-rich sequences known as imprinting control region (ICR). A hexanucleotide motif (TGCCGC), which has an average of two copies per locus, is present in all murine ICRs and is responsible for the methylation-dependent recruitment of ZFP57, which is necessary for the maintenance of DNA methylation at ICRs [48]. This motif is also found in some human ICRs. In this study, a CpG island with six TGCCGC sequences was found in exon 1 of the porcine *XIST* gene, which contained 27 CG dinucleotides (Fig. S4). We analyzed the methylation status of the 27 CpG sites in both male and female fibroblasts. In female cells, the total methylation rate is close to 45%, half of which is hypermethylated and the other half is hypomethylated (Fig. 5a). However, the total methylation rate for male fibroblasts was ~ 98%, corresponding to the X chromosome that does not express *XIST* in male cells (Fig. 5b). This methylation is
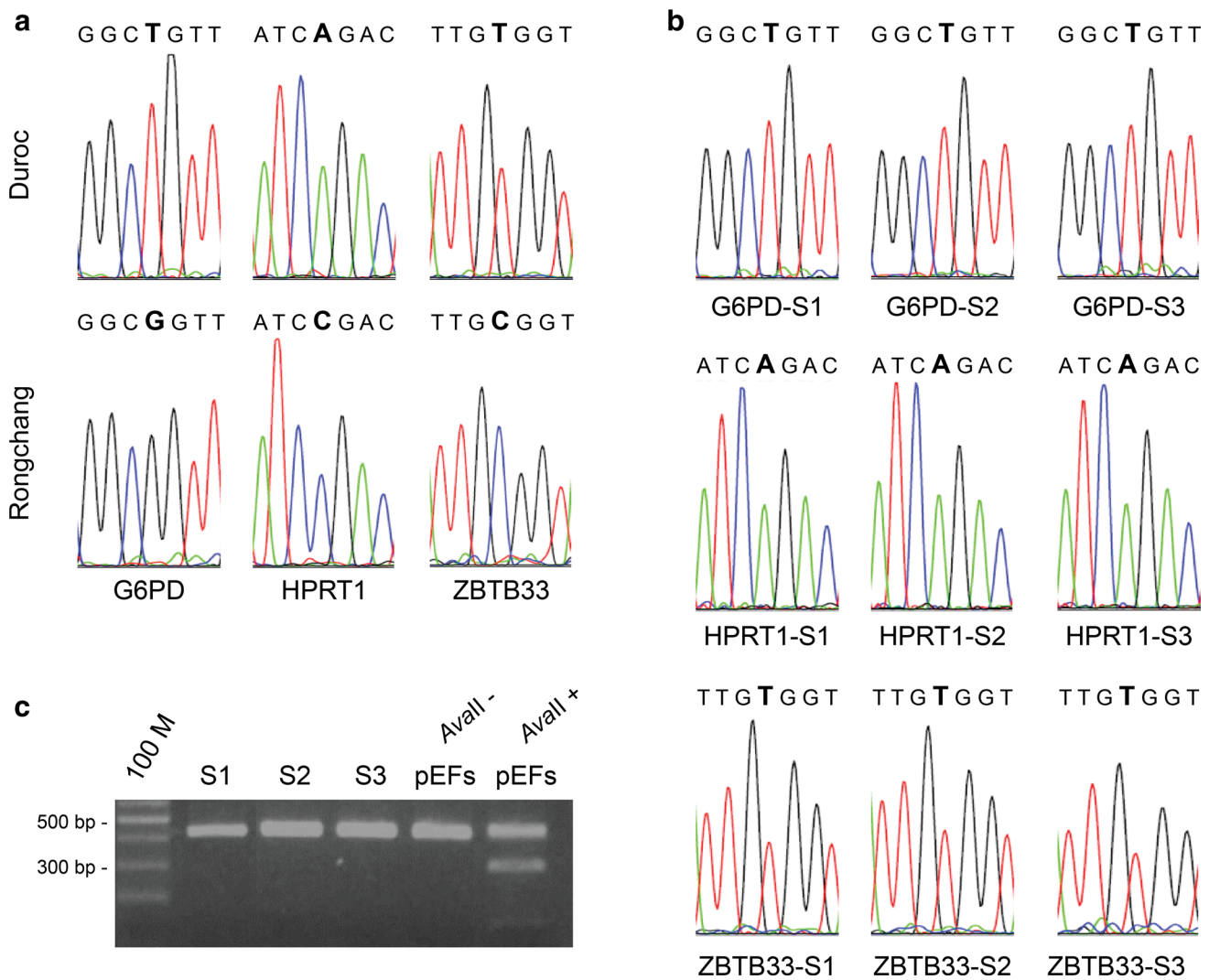
Fig. 2 Three X-linked genes in pigs subjected to XCI. **a** Sequence chromatograph of Rongchang and Durco pigs near the SNP of the *G6PD*, *HPRT1,* and *ZBTB33* genes. Different single peaks represent a nucleotide transition (enlarged letter). **b** The *G6PD*, *HPRT1*, and *ZBTB33* genes in three clonal cell lines (S1, S2, and S3), in which XCI is nonrandom. All three clonal cell lines inactivate the X chromosome from Rongchang, as the *G6PD*, *HPRT1*, and *ZBTB33* genes expressed in three clonal cell lines are from the Duroc allele. **c** Digestion of RT-PCR products of the *XIST* gene in three clonal cell lines. Three clonal cell lines express *XIST* from the Rongchang allele, which is negatively correlated with *G6PD*, *HPRT1,* and *ZBTB33*. pEFs is established from hybrids of Duroc sow and Rongchang boar

characterized by the fact that in female cells, one X chromosome expresses *XIST* while the other does not, suggesting that the analyzed CpG islands were differentially methylated in male and female somatic cells, and are, therefore, defined as a differential methylated region (DMR). We next investigated the DMR methylation status in gametes and found that both sperm and oocyte showed hypomethylation at the CpG islands, and no differential methylation was observed between the gametes (Fig. 5c, d). Developmental analysis of *XIST* DMR methylation in PA embryos, ICSI embryos, and blastocysts in vivo showed that hypomethylation of the CpG islands was maintained to the E7 blastocyst stage (Figs. 5e and S5). The methylation status of the *XIST* CpG islands in

gametes and early embryos was correlated, with no methylation pre-deposited on *XIST* in porcine early embryos.

Discussion

Two approaches have been taken to identify imprinted genes: allele-specific expression analysis and the parthenogenetic model [49]. The paternally imprinted *XIST* expression of mice is determined by allele-specific expression analysis during early embryogenesis [50]. The laboratory mouse model is the most convenient model system for allele-specific expression analysis, as a wealth of different SNPs has
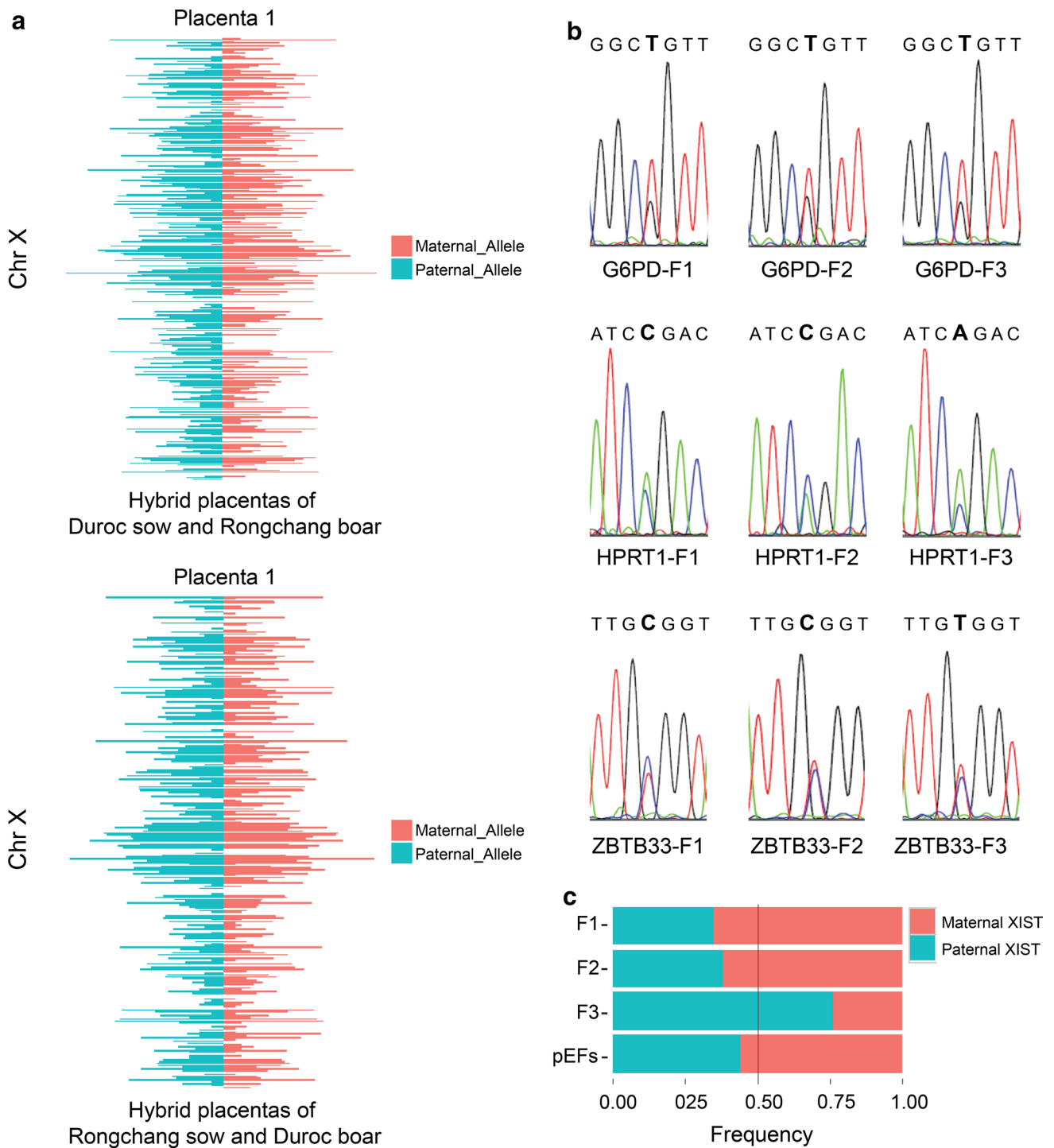
Fig. 3 Biallelic expression of X-linked genes in hybrid placentas. **a** Transcriptome-wide distribution of allele-specific expression in E20 hybrid placentas for X-linked genes. The upper figure is the analysis of RNA-seq data analysis of one E20 female hybrid placenta of Duroc sow and Rongchang boar. Lower panel is RNA-seq data analysis of one E20 female hybrid placenta of Rongchang sow and Duroc boar. The expression ratios of maternal and paternal X chromosome for X-linked genes are nearly 1:1. **b** The expression of *G6PD*, *HPRT1*, and *ZBTB33* in the placentas of three female hybrids (F1, F2 and F3). The X-linked genes of female hybrids are expressed from both alleles, which indicates that random XCI occurs in these placentas. **c** Analysis of *XIST* expression ratios of both alleles in female hybrid placentas (F1, F2 and F3) of Duroc sow and Rongchang boar by TA cloning. Porcine embryonic fibroblast (pEF) is established from hybrids of Duroc sow and Rongchang boar
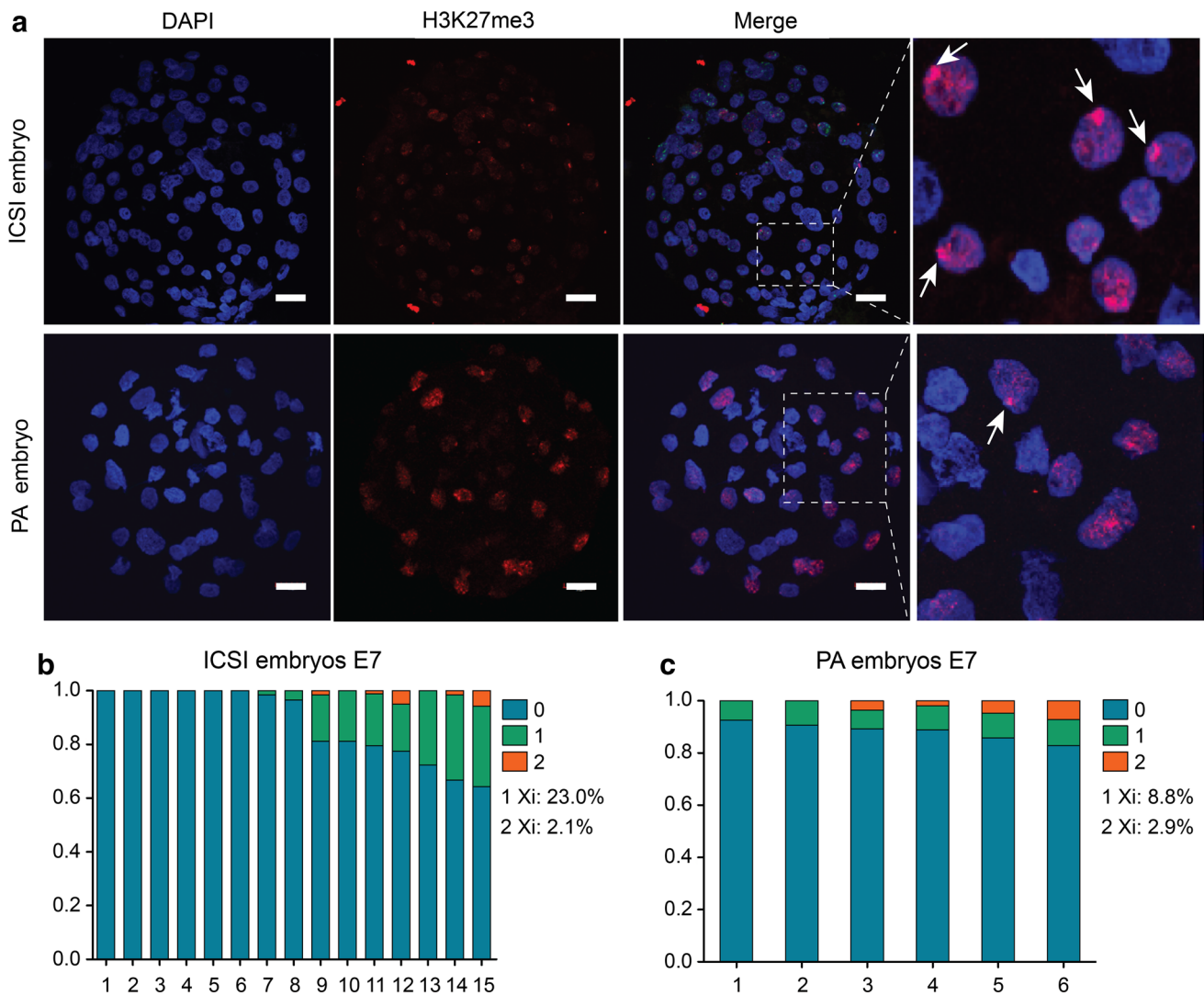
Fig. 4 The XCI status in ICSI and parthenogenetic embryos at E7. **a** Immunostaining of H3K27me3 in ICSI and parthenogenetic embryos. H3K27me3 spots are detected in two types of embryos, each containing different percentages 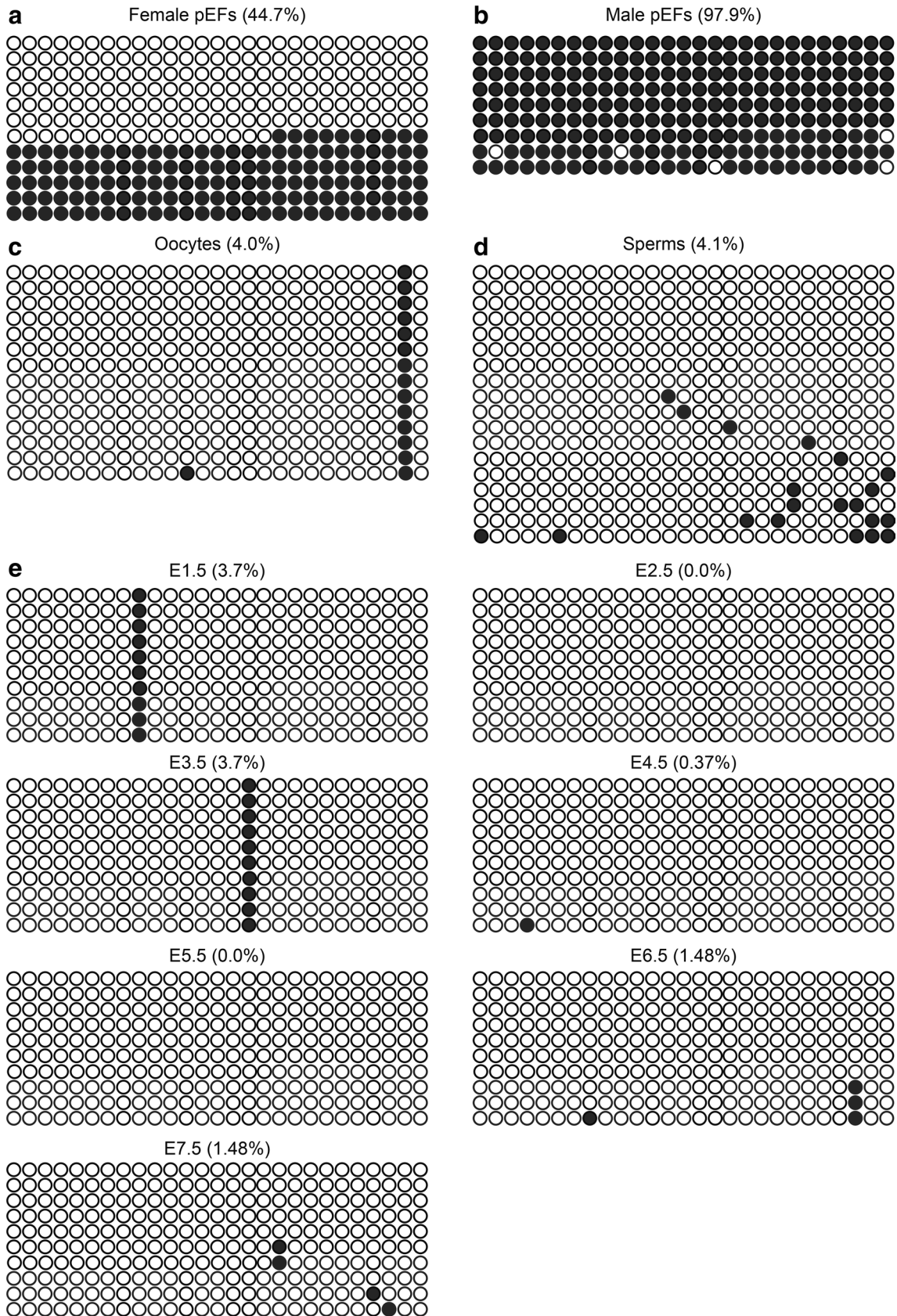of spot cells. White arrowheads indicate the Xi. Scale bars, 20 μm. **b** Percentage of cells containing different numbers of Xi in ICSI embryos. **c** Percentage of cells containing different number of Xi in parthenogenetic embryos

been identified among inbred strains [51]. It is significantly more difficult to identify key genetic markers in other species, typically due to the absence of available inbred animal lines. In this study, we identified a polymorphic marker of the *XIST* gene between Asian- and Western-origin pigs, and used this marker to determine the allele-specific expression status of the *XIST* gene in early porcine embryos.

Both the paternal and maternal alleles of *XIST* transcripts were detected in all female ICSI blastocysts, indicating a different XCI pattern compared to that in mice. In normally fertilized mouse embryos, the paternal allele first begins to express *XIST* from the two-cell stage, indicative of imprinted expression; the maternal *XIST* allele is not expressed until just before gastrulation [52]. In mouse PA embryos, delayed onset of *XIST* expression was found relative to normal

Fig. 5 Analysis of DMR in porcine *XIST*. **a** *XIST* methylation of ▶ female pEFs. The *XIST* gene had two main methylation patterns in female pEFs: completely methylated and completely unmethylated. **b** *XIST* methylation of male pEFs. Hypermethylation of the *XIST* gene in male pEFs. **c** *XIST* methylation in oocytes. *XIST* is hypomethylated in oocytes. **d** *XIST* methylation in sperms. *XIST* was hypomethylated in sperms. **e** *XIST* methylation profile in parthenogenetic embryos. During early development, the *XIST* gene is hypomethylated in parthenogenetic embryos. Each circle represents a CpG dinucleotide. The methylation level (%) was based on the methylated CpGs/all examined CpGs; open circles represent unmethylation and filled circles represent methylation

controls, and *XIST* RNA expression was observed from the morula stage onwards [53]. However, no delayed onset of *XIST* expression was found in porcine PA embryos relative to IVF embryos controls and *XIST* RNA expression was first

a   Female pEFs (44.7%)

b   Male pEFs (97.9%)

c   Oocytes (4.0%)

d   Sperms (4.1%)

e   E1.5 (3.7%)

E2.5 (0.0%)

E3.5 (3.7%)

E4.5 (0.37%)

E5.5 (0.0%)

E6.5 (1.48%)

E7.5 (1.48%)

detected at the morula stage in both PA and IVF embryos in pigs [31]. Interestingly, when we performed sequencing analysis to determine whether there was any parent-of-origin bias of *XIST* transcripts expressed in female ICSI embryos, the result showed that the maternal *XIST* allele was preferentially expressed. This was in line with the previous study of normally fertilized and uniparental porcine embryos [31]. However, we could not exclude the potent effects of in vitro manipulation on the results of this study. In a recent study, it was suggested that *XIST* expression in early porcine embryos could be influenced by the in vitro culture environment [29]. Further allele-specific analysis of porcine embryos in vivo is required to determine the parent-of-origin bias of *XIST* expression.

We analyzed the XCI pattern of pig placental tissue from Rongchang and Duroc pig hybrids using RNA sequencing. Most X-linked genes detected were transcribed from both alleles. To explore the XCI pattern in greater detail, allele-specific expression analysis of X-linked genes subject to XCI should be carried out. However, thus far, no X-linked genes subject to XCI have been identified in pigs. Genome comparison of Rongchang and Duroc pig was carried out to identify a vast number of SNPs along the X-chromosome, including *G6PD*, *HPRT1,* and *ZBTB33*, which were found to be subject to XCI in other mammals [54–56]. Further, these three genes were detected to only express from Xa allele in all clonal fibroblast cell lines from Rongchang and Duroc hybrids, indicating that these genes are also subject to XCI in pigs. This result was further confirmed by *XIST* expression, who expressed only from Xi allele in these clonal cell lines. When we tried to examine the expression of more X-linked genes such as *ARAF1*, *BGN*, *MAOA,* and *BEX1*, they were not constant among these cell lines, similar to that previously reported in humans [54]. What is more, we conducted RNA sequencing to analyze X inactivation profile in three clonal fibroblast cell lines, and supplied 122 candidate genes subject to XCI in pigs. The X-chromosome transcriptome of the placenta of hybrid pigs and the allele-specific expression analysis of four conserved X-linked genes, namely, *XIST*, *G6PD*, *HPRT1,* and *ZBTB33,* in a considerable number of samples suggest that porcine placentas undergo random X inactivation, which is in line with biallelic *XIST* expression in ICSI embryos. To our knowledge, ours is the first study to demonstrate that XCI in porcine placentas is random. Our finding suggests that the mechanism of regulation of XCl in pigs and mice is different.

Indeed, when we investigated the H3K27me3 histone pattern during the early embryonic development of ICSI and PA embryos, no visible Xi-like H3K27me3 domain was observed in morulae and early blastocysts (E4), indicating that XCI may not be initiated at this stage. In contrast, XCI occurs in nearly all cells of early mouse blastocysts [14]. In porcine ICSI blastocysts at E7, only a small part of cells have attained XCI. Furthermore, a previous in vivo study reported that strong punctate signals of H3K27me3 could be detected in most of the female epiblasts and TE nuclei of E10 porcine embryos when XCI was established [57]. Recent research also indicated that dosage compensation of X-linked genes was attained in late epiblasts by single-cell analysis [46].

In this study, a DMR with six TGCCGC sequences, usually found in all murine ICRs, was identified at exon 1 of the porcine *XIST* gene, suggesting that the DMR plays an important role in controlling the expression of the porcine *XIST* gene. This was further confirmed by analyzing the DMR methylation status in both female and male pig fibroblast cells in which the *XIST* gene was differentially expressed. However, the DMR was not methylated in gametes and early embryos, and this finding is consistent with the biallelic *XIST* expression in porcine blastocysts, unlike the case in mice. There is evidence indicating that the paternally imprinted expression of *XIST* in mice early embryos is controlled by differential methylation established during germ cell development [58].

In conclusion, our findings revealed that *XIST* is not imprinted in pigs. The mechanisms regulating XCI in pigs were different from those in mice. Further studies are needed to determine the role of critical regulators of XCI, such as *XACT* [59], *TSIX* [60], *JPX* [61], and *RNF12* [62], and core pluripotency factors [63] during early porcine embryo development. Understanding the mechanisms of XCI would favor the derivation and maintenance of naïve-like ESCs/iPSCs in pigs.

Author contributions HBZ, SW, and NL designed the research; HYZ, DWY, XGD, JW, LC, YYW, HTX, YXZ, SJZ, YWP, YL, HSH, XMZ, WHD, and YPD performed the experiments and analyzed data. HBZ, SW, HYZ, DWY, XGD, and JW wrote the paper. All authors read and approved the final manuscript.

Compliance with ethical standards

References

1. Deng X, Berletch JB, Nguyen DK, Disteche CM (2014) X chromosome regulation: diverse patterns in development, tissues and disease. Nat Rev Genet 15:367–378
2. Lyon MF (1961) Gene action in the X-chromosome of the mouse (Mus musculus L.). Nature 190:372–373
3. Monk M, Harper MI (1979) Sequential X chromosome inactivation coupled with cellular differentiation in early mouse embryos. Nature 281:311–313

4. Tan SS, Williams EA, Tam PPL (1993) X-chromosome inactivation occurs at different times in different tissues of the postimplantation mouse embryo. Nat Genet 4:320

5. Brockdorff N, Turner BM (2015) Dosage compensation in mammals. Cold Spring Harb Perspect Biol 7:a019406

6. Takagi N, Sasaki M (1975) Preferential inactivation of the paternally derived X chromosome in the extraembryonic membranes of the mouse. Nature 256:640–642

7. Penny GD, Kay GF, Sheardown SA, Rastan S, Brockdorff N (1996) Requirement for Xist in X chromosome inactivation. Nature 379:131–137

8. Augui S, Nora EP, Heard E (2011) Regulation of X-chromosome inactivation by the X-inactivation centre. Nat Rev Genet 12:429–442

9. Sahakyan A, Yang Y, Plath K (2018) The role of Xist in X-chromosome dosage compensation. Trends Cell Biol. https://doi.org/10.1016/j.tcb.2018.05.005

10. Galupa R, Heard E (2015) X-chromosome inactivation: new insights into cis and trans regulation. Curr Opin Genet Dev 31:57–66

11. Bonora G, Disteche CM (2017) Structural aspects of the inactive X chromosome. Philos Trans R Soc Lond B Biol Sci 372:20160357. https://doi.org/10.1098/rstb.2016.0357

12. Brockdorff N (2017) Polycomb complexes in X chromosome inactivation. Philos Trans R Soc Lond B Biol Sci 372:20170021. https://doi.org/10.1098/rstb.2017.0021

13. Namekawa SH, Payer B, Huynh KD, Jaenisch R, Lee JT (2010) Two-step imprinted X inactivation: repeat versus genic silencing in the mouse. Mol Cell Biol 30:3187–3205

14. Okamoto I, Otte AP, Allis CD, Reinberg D, Heard E (2004) Epigenetic dynamics of imprinted X inactivation during early mouse development. Science 303:644–649

15. Oikawa M, Inoue K, Shiura H, Matoba S, Kamimura S et al (2014) Understanding the X chromosome inactivation cycle in mice: a comprehensive view provided by nuclear transfer. Epigenetics 9:204–211

16. Borensztein M, Okamoto I, Syx L, Guilbaud G, Picard C et al (2017) Contribution of epigenetic landscapes and transcription factors to X-chromosome reactivation in the inner cell mass. Nat Commun 8:1297

17. Pontier DB, Gribnau J (2011) Xist regulation and function eXplored. Hum Genet 130:223–236

18. Wake N, Takagi N, Sasaki M (1976) Non-random inactivation of X chromosome in the rat yolk sac. Nature 262:580–581

19. Xue F, Tian XC, Du F, Kubota C, Taneja M et al (2002) Aberrant patterns of X chromosome inactivation in bovine clones. Nat Genet 31:216–220

20. Bermejo-Alvarez P, Rizos D, Rath D, Lonergan P, Gutierrez-Adan A (2010) Sex determines the expression level of one third of the actively expressed genes in bovine blastocysts. Proc Natl Acad Sci USA 107:3394–3399

21. Wang X, Miller DC, Clark AG, Antczak DF (2012) Random X inactivation in the mule and horse placenta. Genome Res 22:1855–1863

22. Tachibana M, Ma H, Sparman ML, Lee HS, Ramsey CM et al (2012) X-chromosome inactivation in monkey embryos and pluripotent stem cells. Dev Biol 371:146–155

23. Petropoulos S, Edsgard D, Reinius B, Deng Q, Panula SP et al (2016) Single-cell RNA-seq reveals lineage and X chromosome dynamics in human preimplantation embryos. Cell 167:285

24. Sahakyan A, Kim R, Chronis C, Sabri S, Bonora G et al (2017) Human naive pluripotent stem cells model X chromosome dampening and x inactivation. Cell Stem Cell 20:87–101

25. Moreira de Mello JC, Fernandes GR, Vibranovski MD, Pereira LV (2017) Early X chromosome inactivation during human preimplantation development revealed by single-cell RNA-sequencing. Sci Rep 7:10794

26. Vallot C, Patrat C, Collier AJ, Huret C, Casanova M et al (2017) XACT noncoding RNA competes with XIST in the control of X chromosome activity during human early development. Cell Stem Cell 20:102–111

27. Inoue K, Kohda T, Sugimoto M, Sado T, Ogonuki N et al (2010) Impeding Xist expression from the active X chromosome improves mouse somatic cell nuclear transfer. Science 330:496–499

28. Nichols J, Smith A (2009) Naive and primed pluripotent states. Cell Stem Cell 4:487–492

29. Park CH, Jeong YH, Jeong YI, Lee SY, Jeong YW et al (2012) X-linked gene transcription patterns in female and male in vivo, in vitro and cloned porcine individual blastocysts. PLoS One 7(12):e51398

30. Hwang JY, Kim EB, Ka H, Lee CK (2013) Identification of the porcine XIST gene and its differential CpG methylation status in male and female pig cells. PLoS One 8(9):e73677

31. Park CH, Uh KJ, Mulligan BP, Jeung EB, Hyun SH et al (2011) Analysis of imprinted gene expression in normal fertilized and uniparental preimplantation porcine embryos. PLoS One 6(7):e22216

32. Moreira de Mello JC, de Araujo ES, Stabellini R, Fraga AM, de Souza JE et al (2010) Random X inactivation and extensive mosaicism in human placenta revealed by analysis of allele-specific gene expression along the X chromosome. PLoS One 5:e10947

33. Wang X, Douglas KC, Vandeberg JL, Clark AG, Samollow PB (2014) Chromosome-wide profiling of X-chromosome inactivation and epigenetic states in fetal brain and placenta of the opossum, Monodelphis domestica. Genome Res 24:70–83

34. Cheng HC, Zhang FW, Deng CY, Jiang CD, Xiong YZ et al (2007) NNAT and DIRAS3 genes are paternally expressed in pigs. Genet Sel Evol 39:599–607

35. Groenen MA, Archibald AL, Uenishi H, Tuggle CK, Takeuchi Y et al (2012) Analyses of pig genomes provide insight into porcine demography and evolution. Nature 491:393–398

36. Bischoff SR, Tsai SQ, Hardison NE, Motsinger-Reif AA, Freking BA et al (2013) Differences in X-chromosome transcriptional activity and cholesterol metabolism between placentae from swine breeds from Asian and Western origins. PLoS One 8:e55345

37. Du Y, Kragh PM, Zhang X, Purup S, Yang H et al (2005) High overall in vitro efficiency of porcine handmade cloning (HMC) combining partial zona digestion and oocyte trisection with sequential culture. Cloning Stem Cells 7:199–205

38. Kikuchi K, Nagai T, Kashiwazaki N, Ikeda H, Noguchi J et al (1998) Cryopreservation and ensuing in vitro fertilization ability of boar spermatozoa from epididymides stored at 4 degrees C. Theriogenology 50:615–623

39. Nakai M, Ito J, Sato K, Noguchi J, Kaneko H et al (2011) Pretreatment of sperm reduces success of ICSI in the pig. Reproduction 142:285–293

40. Namekawa SH, Lee JT (2011) Detection of nascent RNA, single-copy DNA and protein localization by immunoFISH in mouse germ cells and preimplantation embryos. Nat Protoc 6(3):270–284

41. Yu D, Wang J, Zou H, Feng T, Chen L et al (2018) Silencing of retrotransposon-derived imprinted gene RTL1 is the main cause for postimplantational failures in mammalian cloning. Proc Natl Acad Sci USA 115:E11071–E11080

42. Wang J, Zou H, Chen L, Long X, Lan J et al (2017) Convergent and divergent genetic changes in the genome of Chinese and European pigs. Sci Rep 7:8662

43. Kim D, Langmead B, Salzberg SL (2015) HISAT: a fast spliced aligner with low memory requirements. Nat Methods 12:357–360

44. Anders S, Pyl PT, Huber W (2015) HTSeq—a Python framework to work with high-throughput sequencing data. Bioinformatics 31:166–169

45. Carrel L, Willard HF (1999) Heterogeneous gene expression from the inactive X chromosome: an X-linked gene that escapes X inactivation in some human cell lines but is inactivated in others. Proc Natl Acad Sci USA 96:7364–7369

46. Ramos-Ibeas P, Sang F, Zhu Q, Tang WWC, Withey S et al (2019) Pluripotency and X chromosome dynamics revealed in pig pregastrulating embryos by single cell analysis. Nat Commun 10:500

47. Zuccotti M, Monk M (1995) Methylation of the mouse Xist gene in sperm and eggs correlates with imprinted Xist expression and paternal X-inactivation. Nat Genet 9:316–320

48. Quenneville S, Verde G, Corsinotti A, Kapopoulou A, Jakobsson J et al (2011) In embryonic stem cells, ZFP57/KAP1 recognize a methylated hexanucleotide to affect chromatin and DNA methylation of imprinting control regions. Mol Cell 44:361–372

49. Bischoff SR, Tsai S, Hardison N, Motsinger-Reif AA, Freking BA et al (2009) Characterization of conserved and nonconserved imprinted genes in swine. Biol Reprod 81:906–920

50. Kay GF, Barton SC, Surani MA, Rastan S (1994) Imprinting and X-chromosome counting mechanisms determine Xist expression in early mouse development. Cell 77:639–650

51. Ferguson-Smith A, Lin SP, Tsai CE, Youngson N, Tevendale M (2003) Genomic imprinting—insights from studies in mice. Semin Cell Dev Biol 14:43–49

52. Kay GF, Penny GD, Patel D, Ashworth A, Brockdorff N et al (1993) Expression of Xist during mouse development suggests a role in the initiation of X-chromosome inactivation. Cell 72:171–182

53. Nesterova TB, Barton SC, Surani MA, Brockdorff N (2001) Loss of Xist imprinting in diploid parthenogenetic preimplantation embryos. Dev Biol 235:343–350

54. Carrel L, Willard HF (2005) X-inactivation profile reveals extensive variability in X-linked gene expression in females. Nature 434:400–404

55. Al Nadaf S, Deakin JE, Gilbert C, Robinson TJ, Graves JA et al (2012) A cross-species comparison of escape from X inactivation in Eutheria: implications for evolution of X chromosome inactivation. Chromosoma 121:71–78

56. Okamoto I, Patrat C, Thepot D, Peynot N, Fauque P et al (2011) Eutherian mammals use diverse strategies to initiate X-chromosome inactivation during development. Nature 472:370–374

57. Gao Y, Hyttel P, Hall VJ (2011) Dynamic changes in epigenetic marks and gene expression during porcine epiblast specification. Cell Reprogr 13:345–360

58. Norris DP, Patel D, Kay GF, Penny GD, Brockdorff N et al (1994) Evidence that random and imprinted Xist expression is controlled by preemptive methylation. Cell 77:41–51

59. Vallot C, Huret C, Lesecque Y, Resch A, Oudrhiri N et al (2013) XACT, a long noncoding transcript coating the active X chromosome in human pluripotent cells. Nat Genet 45:239–241

60. Lee JT (2005) Regulation of X-chromosome counting by Tsix and Xite sequences. Science 309:768–771

61. Sun S, Del Rosario BC, Szanto A, Ogawa Y, Jeon Y et al (2013) Jpx RNA activates Xist by evicting CTCF. Cell 153:1537–1551

62. Gontan C, Achame EM, Demmers J, Barakat TS, Rentmeester E et al (2012) RNF12 initiates X-chromosome inactivation by targeting REX1 for degradation. Nature 485:386–390

63. Navarro P, Chambers I, Karwacki-Neisius V, Chureau C, Morey C et al (2008) Molecular coupling of Xist regulation and pluripotency. Science 321:1693–1695